Laser and Particle Beams (2001), *19*, 111–115. Printed in the USA.

Equation of state of water in the megabar range

E. HENRY,[1,2] D. BATANI,[1] M. KOENIG,[2] A. BENUZZI,[2] I. MASCLET,[3] B. MARCHET,[3]
M. REBEC,[3] CH. REVERDIN,[3] P. CELLIERS,[4] L. DA SILVA,[4] R. CAUBLE,[4]
G. COLLINS,[4] T. HALL,[5] AND C. CAVAZZONI[6]

[1]Dipartimento di Fisica "G. Occhialini," Università degli Studi di Milano–Bicocca and I.N.F.M., Via Emanueli 15, 20146 Milano, Italy
[2]L.U.L.I, C.N.R.S. École Polytechnique, 91128 Palaiseau, France
[3]C.E.A. Limeil, France
[4]Lawrence Livermore National Laboratory, Livermore, CA, U.S.A.
[5]University of Essex, Essex, U.K.
[6]C.I.N.E.C.A., Bologna, Italy

(RECEIVED 30 November 2000; ACCEPTED 5 February 2001)

Abstract

We present some preliminary results on the equation of state (EOS) of water in a pressure regime of astrophysical interest. In the experiments, structured targets made of an aluminum step followed by a water layer are irradiated by the laser at an intensity up to $4 \cdot 10^{14}$ W·cm^{-2} to generate a shock wave. Velocities are measured in the two materials using a VISAR interferometric diagnostic for water, and a streak camera to measure target self-emission for Al. EOS points for water are obtained with the impedance mismatch method using Al EOS as a reference. Water reflectivity was also measured.

1. INTRODUCTION

1.1. Astrophysical context

The mantle of Neptune and Uranus is mainly constituted by "ice layers" containing water, methane, and ammonia. The magnetic field of both planets, as measured by the probe Voyager 2, is larger than what was expected and asymmetrical, originating from the conductivity of those layers. The range of pressure and temperature in the ice layers is 0.2 to 6 Mbar and 2000 K to 8000 K. Estimations of the minimum conductivity capable of sustaining the magnetic field by dynamo effect give about 200 $(\Omega \cdot \mathrm{cm})^{-1}$. Recent calculations predict a transition from electrolyte to metal in this regime for water and ammonia (Cavazzoni *et al.*, 1999). Yet no measure has so far confirmed its existence.

1.2. Goals of our experiment

We describe here the first experiments measuring the equation of state (EOS) of water with laser-driven shock waves in the pressure range of 1–10 Mbar. This technique of measurement has been much improved in recent years (Koenig *et al.*, 1995) and has become a reliable tool for high pressure physics (Zeldovich & Raizer, 1967). The first experiments were conducted at the Commissariat à l'Énergie Atomique in Limeil, France, and completed later on by experiments on the LULI laser, at the École Polytechnique, France. Both were funded by the European Union in the framework of the "Access to Large Scale Facilities" program. Our goals were to obtain new experimental points for the EOS of water in the megabar range, as well as to estimate the conductivity in this range of pressures.

2. EXPERIMENTAL SETUP

The experiments are based on the impedance mismatch method, where the shock velocity is simultaneously measured in two different materials, one of which is used as a reference. We chose aluminum, as its EOS is well known up to 40 Mbar (*Sesame*, 1992). As both experiments are very similar, we only describe the setup for the experiment performed at LULI. The parameters for each setup are compared in Table 1.

We used three beams of the LULI laser (cf. Fig. 1a) in the green, optically smoothed with phase zone plates (PZP), and focused on the target (cf. Fig. 1b). A probe beam with a longer duration and very little energy (a few millijoules) was reflected on the rear side of the target. The reflected beam was sent to two VISAR (velocity interferometer sys-

Address correspondence and reprint requests to: Emeric Henry, Dipartimento di Fisica "G. Occhialini," Università degli Studi di Milano–Bicocca, Via Emanueli 15, 20126 Milano, Italy. E-mail: Emeric.Henry@fisica.unimi.it

Table 1. *Experimental parameters for the Limeil and LULI setups*

	Limeil	LULI
High-power laser		
Wavelength λ	0.532 μm	0.532 μm
Square pulse duration	4ns	600 ps
Maximum energy	2000 J	100 J
Optical smoothing	Kinoform phase plate	Phase zone plate
Focal spot	900×600 μm^2	400×400 μm^2
Maximum intensity	1.4×10^{14} W·cm^{-2}	8×10^{13} W·cm^{-2}
Probe beam		
Wavelength λ	1.064 μm	0.537 μm
Gaussian pulse duration	10 ns	8 ns

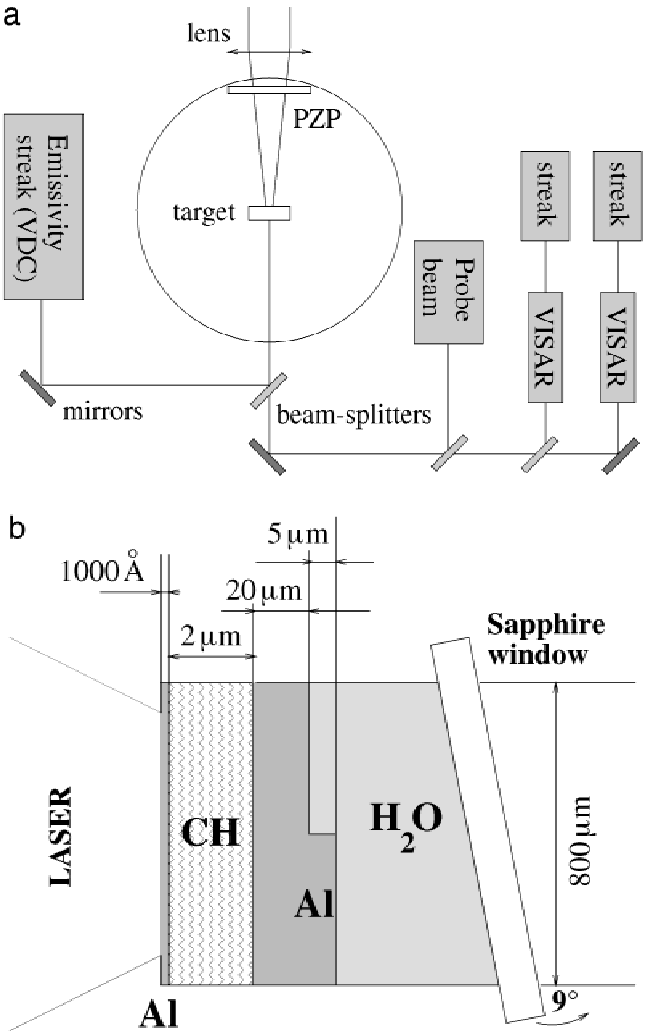

Fig. 1. Experimental setup and water targets for the LULI experiment. (a) Setup: The high-power laser beam is optically smoothed by PZP and focused on the target; a probe beam is reflected on its rear side and analyzed by two velocity interferometers (VISAR) with different sensitivities; the emissivity of the target is recorded by a third diagnostic. (b) Target: A layer of CH is used to minimize preheating ahead of the shock, and a thin Al foil avoids laser shine-through at early times. The Al layer includes a step of thickness $h = 5$ μm.

tems for any reflector; Celliers *et al.*, 1998), velocity interferometers which measure the velocity of the rear side of the target: The Doppler effect at the reflecting surface induces a shift in wavelength for the probe beam, hence modifying the interference pattern. The sideways shift of the fringes is proportional to the velocity of the reflecting surface. To resolve the ambiguity on the initial shift of the fringes at the shock arrival (Trunin, 1994), we used two VISARs with different sensitivities (16.7 km·s^{-1} and 3.4 km·s^{-1} per fringe, respectively) coupled with streak cameras. Assuming that water is metallized, the probe beam crosses "cold" water and gets reflected on the shock front. Evaluating the Doppler effect at the interface brings about a modification of the usual VISAR formula (Barker, 1972) involving the refractive index of "cold" water n at the wavelength λ of the probe beam:

$$V(t) = F(t)\,\frac{\lambda}{2\tau c n}, \tag{1}$$

where $F(t)$ is the fringe shift, τ the delay introduced by the interferometer, and $V(t)$ the velocity measured.

To image the rear side of the target, we used an image relaying system to avoid vignetting (i.e., a luminosity drop on the borders of the image). The two streak cameras coupled with the VISAR had a spatial resolution of 4 μm and a temporal resolution of 10 ps. A third streak camera with a temporal resolution of 4 ps was used to record the target self-emission (VDC).

The targets consist of an aluminum step of height h (typically a few microns) and a cell filled with water (cf. Fig. 1b). To minimize preheating of the target, a layer of plastic (CH) was added on the front side; finally, a very thin Al foil was placed to avoid laser shine-through at early times.

3. EXPERIMENTAL RESULTS

The transit time Δt of the shock in the aluminum step is measured with the VDC: When the shock breaks through, Al begins to emit, and a visible signal is detected (Fig. 2a). This measurement is confirmed with the VISARs (Fig. 2b and 2c). Hence, knowing the thickness h of the step (and assuming that the shock is stationary—cf. Fig. 3a), the shock velocity in Al can be simply calculated as $D_{\mathrm{Al}} = h/\Delta t$.

The use of the VISARs' diagnostics can only be done if we know where the probe beam gets reflected. If water is not metallized, the probe beam crosses compressed, ionic water and is reflected by the Al layer. In this case, the VISARs measure the fluid velocity. If, on the other hand, water is metallized, it reflects the probe beam, and we measure the velocity of the shock front.

For all our shots, we could say that the probe beam was reflected on metallized water. Indeed, calculations by Cavazzoni (2000) predict that the Hugoniot curve reaches the

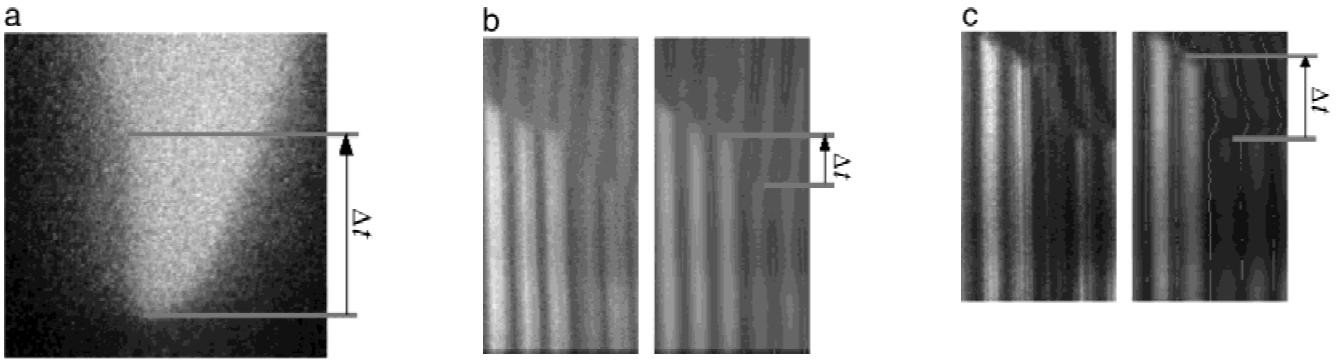

Fig. 2. Experimental images from shot #60: (a) Target self-emission: We measure the transit time Δt of the shock in the Al step. (b,c) Images from the two VISARs and the processed images: We measure the fringe shift, get an independent measurement of the shock transit time in the Al step, and measure the reflectivity of the target.

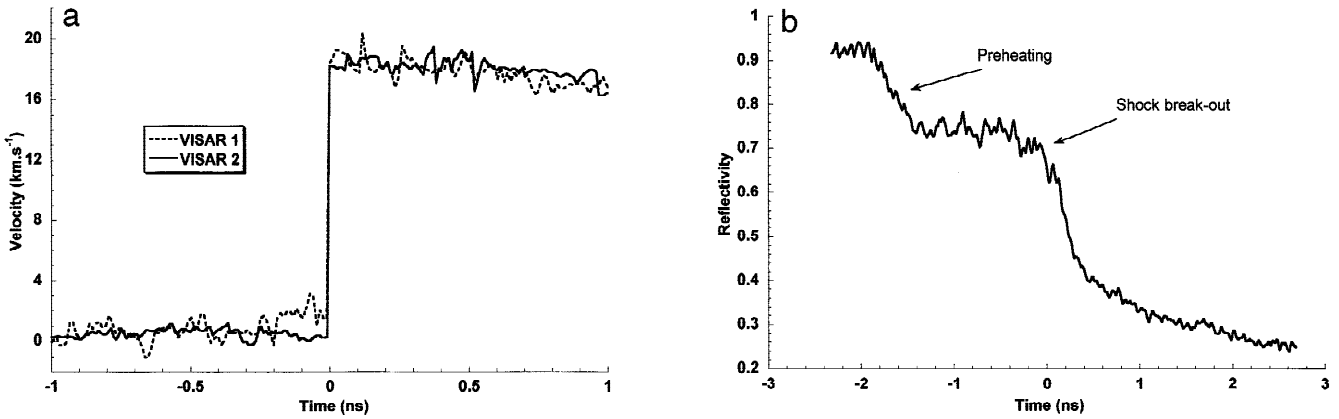

Fig. 3. Measurements from shot #60: (a) Shock velocity profile measured with the VISARs from the images of Figure 2b. The shock remains stationary for about 1 ns. (b) Reflectivity of the target measured from the images of Figure 2b. Initially, the reflectivity decreases because of a small preheating of the target. Immediately after the shock breakout, its value is about 0.45.

metallic state above approximately 1 Mbar. Moreover, the high reflectivity measured indicates the metallization of water. Finally, assuming that water was *not* metallized leads to EOS points very far from the Sesame table (*Sesame*, 1992), or even in regions that are not physically possible (such as negative density).

The shock velocity in water is thus measured by the fringe shift on the VISARs (cf. Fig. 2b and 2c). We used an image processing code to reconstruct the interference pattern from the sometimes noisy images.

Once we have measured two parameters—the shock velocity in Al and water—we can use the impedance mismatch method: When the shock arrives at the interface between Al and water, a shock is transmitted in water and a relaxation wave propagates backwards in Al. As the EOS of Al is well known, we can compute the parameters of the relaxation wave in Al. Then, stating that pressure and fluid velocity have to be equal on each side of the interface, we obtain a point on the EOS of water. The results for the EOS are shown in Table 2 and Fig. 4; the agreement with the Sesame table (*Sesame*, 1992) is good.

In our experiment we also measured the reflectivity of the interface between metallized and "cold" water by comparing the signal from shocked and unperturbed regions of the target (cf. Fig. 3b). High reflectivities of the order of 50% are observed.

Table 2. *Experimental results*

Shot #	D Al ($km \cdot s^{-1}$)	D water ($km \cdot s^{-1}$)	P water (Mbar)	Conductivity σ ($\Omega \cdot cm^{-1}$)
59	18.7	19.2	2.7	
60	18.15	18.5	2.4	
61	14.4	15.3	1.4	
63	12.5	10.7	0.8	7×10^3
65	19.6	20.9	3.1	2.5×10^3
66	17.2	19.1	2.3	2.7×10^3
67	11.8	11.3	0.8	2×10^4
L1	20.3	26.1	3.8	2×10^3
L2	19.4	25.9	3.6	2×10^3

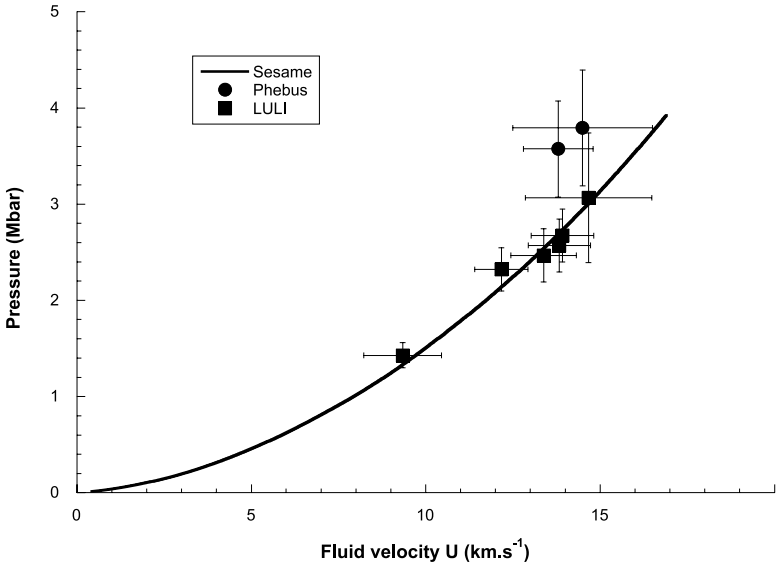

Fig. 4. Experimental points for the EOS of water and comparison with the Sesame table (*Sesame*, 1992).

From the experimentally measured reflectivity, electromagnetism allows calculating the conductivity of metallized water. This conductivity is of electronic nature, as it is the response to an optical signal (i.e., of typical frequency 10^{15} Hz). Results are shown in Figure 5a and 5b. Conductivities of the order of $10^3\ \Omega\cdot\mathrm{cm}^{-1}$ are observed, well in agreement with the hypothesis of water metallization.

We also observe a decrease in conductivity as pressure increases, and this can be fairly well reproduced by a semiclassical formula for conductivity:

$$\sigma \propto \frac{\rho^{2/3} Z^*}{\sqrt{T}}, \tag{2}$$

where the degree of ionization Z^* has been computed with the Thomas–Fermi model (cf. Fig. 5b).

4. CONCLUSIONS

The results presented here are the first measurement of the EOS of water with laser-driven shock waves. This method proved to be a reliable tool for this measurement, as new points have been obtained in good agreement with previous data. We found evidence of a high electronic conductivity of water at $P \geq 1.4$ Mbar and $T \geq 0.9$ eV, in good agreement with calculations by Cavazzoni (2000) which predict the transition from ionic to metallic conductor above about 1 Mbar along the Hugoniot curve.

ACKNOWLEDGMENT

This work was supported by European Programmes E.U.TMR, under the contract ERBFMGECT 950016.

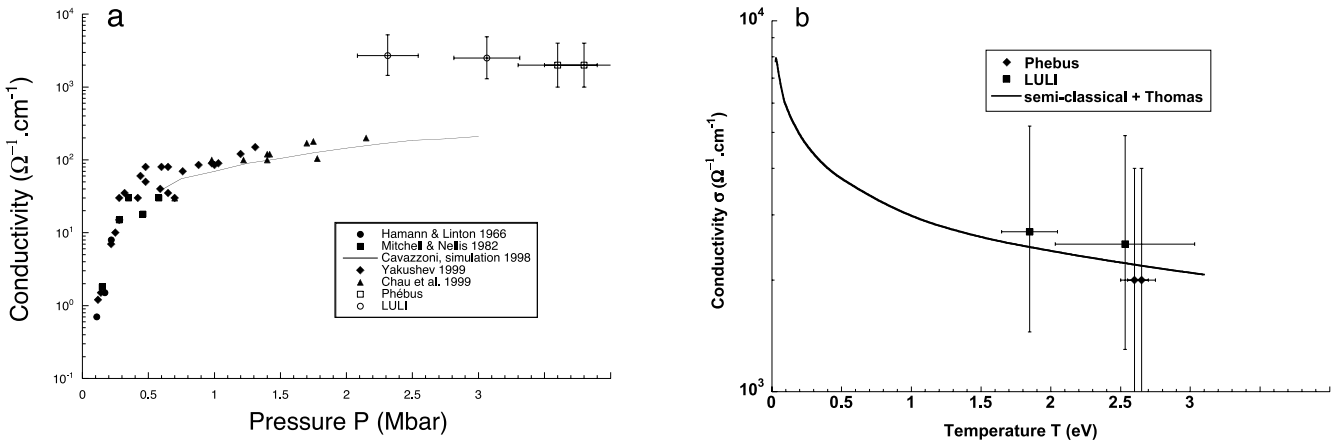

Fig. 5. Estimation of the conductivity: (a) Comparison with measurements of the conductivity along an isentrope. (b) Comparison with a semiclassical formula for conductivity, where ionization is computed with the Thomas–Fermi model.

REFERENCES

Barker, L.M. (1972). Laser interferometer for measuring high velocities of any reflecting surface. *J. Appl. Phys.* **43**, 4669–4675.

Cavazzoni, C. (2000). Calculation of Hugoniot points for water. Unpublished.

Cavazzoni, C., Chiarotti, G.L., Scandolo, S., Tosatti, M., Bernasconi, E. & Parrinello, M. (1999). Superionic and metallic states of water and ammonia at giant planet conditions. *Science* **283**, 44–46.

Celliers, P.M., Collins, G.W., Da Silva, L.B., Gold, D.M. & Cauble, R. (1998). Accurate measurement of laser-driven shock trajectories with velocity interferometry. *Applied Phys. Lett.* **73**, 1320–1322.

Chau, R., Mitchell, A.C., Minich, R.W. & Nellis, W.J. (2001). Electrical conductivity of water compressed dynamically to pressures of 70–180 GPa (0.7–1.8 Mbar). *Journal of Chemical Physics* **114**, 1361.

Koenig, M., Faral, B., Boudenne, J.M., Batani, D., Benuzzi, A., Bossi, S., Rémond, C., Perrine, J., Temporal, M. & Atzeni, S. (1995). Relative consistency of equations of state by laser driven shock waves. *Phys. Rev. Lett.* **74**, 2260–2263.

Mitchell, A.C. & Nellis, W.J. (1982). Equation of state and electrical conductivity of water and ammonia shocked to the 100 GPa (1 Mbar) range. *Journal of Chemical Physics* **76**, 6273.

Sesame. (1992). Report LA-UR-92-3407, Los Alamos National Laboratory.

Trunin, R.F. (1994). Shock compressibility of condensed materials in strong shock waves generated by underground nuclear explosions. *Phys.-Usp.* **37**, 1123–1145, or *Uspekhi Fizicheskii Nauk* **164**, 1215–1237.

Yakushev, V.V., Postnov, V.I., Fortov, V.E. & Yakysheva, T.I. (2000). Electrical conductivity of water during quasi-isentropic compression to 130 GPa. *Journal of Experimental and Theoretical Physics* **117**, 710.

Zeldovich, Y.B. & Raizer, Y.P. (1967). *Physics of shock waves and high temperature hydrodynamic phenomena* (Academic Press, New York).